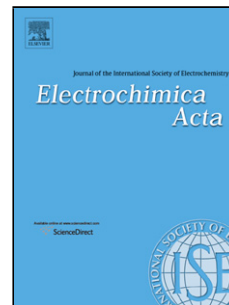


Accepted Manuscript

Title: T-shaped (D)₂-A- π -A type sensitizers incorporating indoloquinoxaline and triphenylamine for organic dye-sensitized solar cells

Authors: Xing Qian, Xiaolin Lan, Rucai Yan, Yiming He, Jiazheng Huang, Linxi Hou



PII: S0013-4686(17)30446-2
DOI: <http://dx.doi.org/doi:10.1016/j.electacta.2017.02.166>
Reference: EA 29031

To appear in: *Electrochimica Acta*

Received date: 5-1-2017
Revised date: 26-2-2017
Accepted date: 27-2-2017

Please cite this article as: Xing Qian, Xiaolin Lan, Rucai Yan, Yiming He, Jiazheng Huang, Linxi Hou, T-shaped (D)₂-A- π -A type sensitizers incorporating indoloquinoxaline and triphenylamine for organic dye-sensitized solar cells, *Electrochimica Acta* <http://dx.doi.org/10.1016/j.electacta.2017.02.166>

This is a PDF file of an unedited manuscript that has been accepted for publication. As a service to our customers we are providing this early version of the manuscript. The manuscript will undergo copyediting, typesetting, and review of the resulting proof before it is published in its final form. Please note that during the production process errors may be discovered which could affect the content, and all legal disclaimers that apply to the journal pertain.

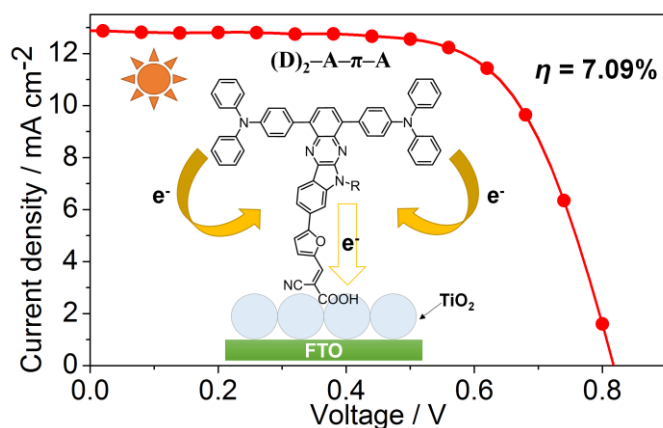
T-shaped (D)₂-A- π -A type sensitizers incorporating indoloquinoline and triphenylamine for organic dye-sensitized solar cells

Xing Qian, Xiaolin Lan, Rucai Yan, Yiming He, Jiazheng Huang, Linxi Hou*

College of Chemical Engineering, Fuzhou University, Xueyuan Road No. 2, Fuzhou
350116, China

*Corresponding author. E-mail address: lxhou@fzu.edu.cn.

Graphical Abstract



Highlights:

1. Four novel T-shaped $(D)_2-A-\pi-A$ type organic dyes have been synthesized.
2. Two triphenylamine donors and an indoloquinoxaline acceptor were combined.
3. Different acceptors and π -bridges were used to tune the photoelectric properties.
4. A highest PCE of 7.09% was achieved by the dye **QX23**.

Abstract: Four novel T-shaped metal-free organic sensitizers **QX22–25** based on triphenylamine and indoloquinoxaline have been successfully designed and synthesized as a $(D)_2-A-\pi-A$ type structure. These dye sensitizers have two triphenylamine donors attaching on an indoloquinoxaline-based subordinate acceptor. Different π -bridges (thiophene and furan) and acceptor/anchoring groups (cyanoacrylic acid and 2-(1,1-dicyanomethylene)rhodanine) were involved to tune the

photoelectrical properties. Their optical, electrochemical, and photovoltaic properties as well as the DFT calculations have been systematically investigated, indicating these four dyes are all capable as photosensitizers. A highest power conversion efficiency up to 7.09% with a J_{sc} of 12.9 mA cm⁻² and a V_{oc} of 817 mV has been achieved by the dye **QX23** with a furan π -bridge and a cyanoacrylic acid acceptor/anchoring group, indicating it is a promising strategy to construct efficient (D)₂-A- π -A type sensitizers by incorporating indoloquinoline and triphenylamine.

Keywords: Dye-sensitized solar cells; Organic sensitizers; Triphenylamine; Indoloquinoline; (D)₂-A- π -A structure

1. Introduction

Dye-sensitized solar cells (DSSCs) as promising photoelectric devices have shown great potential due to their high power conversion efficiency (PCE) and low cost of production [1,2]. A typical DSSC contains a semiconductor photoanode, an electrolyte, a counter electrode, and a dye sensitizer [3–5]. In DSSC devices, dye sensitizers play a key role on capturing sunlight, transferring charge, and injecting electron into photoanode [6–10]. To date, a landmark PCE of 13% have been reported for zinc porphyrin-based DSSC under AM 1.5G illumination [11]. Compared with the well-known efficient porphyrin sensitizers, more and more attention has been devoted in developing the metal-free organic sensitizers recently owing to their low cost, easy

synthetic progress, and high yields [12–16].

Donor- π -acceptor (D- π -A) type structure is the common conformation for most organic sensitizers because of their promoted intramolecular charge transfer (ICT) [17–21]. Recently, the D-A- π -A type structure with an additional acceptor involved into the conventional D- π -A structure was intensively reported and received increasing attention [22–26]. Through inserting a subordinate acceptor acting as the electron trap to promote charge separation and facilitate electron transfer to the final acceptor, the D-A- π -A type sensitizers exhibit broad responsive spectra and long term photo-stability [27]. A series of electron-withdrawing groups such as quinoxaline [28–30], benzothiadiazole [31–34], benzotriazole [35,36], benzoxadiazole [37], and diketopyrrolopyrrole [38,39] etc. have been incorporated into the D-A- π -A type sensitizers to conveniently tune the molecular energy level and modulate the light-harvesting response range.

Herein, we report a novel T-shaped (D)₂-A- π -A type structure with double triphenylamine donors and a indoloquinoxaline as the subordinate acceptor. Triphenylamine containing an electron-rich nitrogen atom also has a nonplanar propeller conformation in the ground state, which can suppress the intermolecular aggregations. Thus, triphenylamine is widely used as the donor part for metal-free organic sensitizers in DSSCs due to its unique electronic and optical properties [40–43]. On the other hand, 6*H*-indolo[2,3-*b*]quinoxaline contains an electron-deficient quinoxaline which is fused with an electron-rich indole unit and it can be considered as a rigid planar built-in donor-acceptor chromophore [44]. This

unique dipolar structure endows indoloquinoxaline with an excellent natural potential for ICT process [45]. On this research, our strategy is to introduce two triphenylamine donors attached on an indoloquinoxaline acceptor to form a T-shaped (D)₂-A structure and to combine the advantages of triphenylamine and indoloquinoxaline. This (D)₂-A moiety can be used to connect with the π -A moiety to form a (D)₂-A- π -A system. Based on their strong ICT characteristic and high synthetic flexibility of triphenylamine and indoloquinoxaline, we have designed and synthesized four new organic dyes **QX22–25**. Different acceptors (cyanoacetic acid with a -COOH anchoring group and 2-(1,1-dicyanomethylene)rhodanine, DCRD, without a -COOH anchoring group) and different π -bridges (thiophene and furan) have been investigated to further tune the photoelectric properties of these dyes. The chemical structures of the four dyes are shown in Fig. 1.

2. Experimental section

2.1. Materials and instruments

All reagents were obtained from Sigma-Aldrich, TCI and Alfa aesar. All solvents were used after being purified through common standard purification methods. FTO conductive glasses (a sheet resistance of 15 Ω sq⁻¹, Nippon Sheet Glass) were used. The ¹H and ¹³C NMR measurements were performed on a Bruker 400 MHz spectrometer. The UV-vis absorption spectra of all dyes were recorded on a UV-vis spectrophotometer (Varian Cary 300 Conc). HR-MS data were recorded on a Varian 7.0T FTMS system. Cyclic voltammetry (CV) and electrochemical impedance

spectroscopy (EIS) tests were performed using an electrochemical workstation (CHI660E, CH Instrument). CV measurements were conducted using a three-electrode system with a glassy carbon electrode as the working electrode, an Ag/Ag⁺ electrode as the reference electrode, and a platinum plate as the counter electrode. The redox potentials were recorded in dichloromethane (DCM) solutions using 0.1 M tetrabutylammonium hexafluorophosphate (*n*-Bu₄NPF₆) as the supporting electrolyte with a scan rate of 100 mV S⁻¹.

2.2. Fabrication and Characterization of DSSCs

The TiO₂ photoanodes were prepared according to our previous works [46]. A transparent nanocrystalline TiO₂ film (~12 μm) and a scattering layer (~4 μm) were prepared over FTO glasses by screen-printing method. Afterwards, the electrodes were gradually heated to 500 °C and sintered for 1 hour. Then, the prepared electrodes were treated with 0.04 M TiCl₄ aqueous solution at 70 °C for 1 hour and sintered again at 500 °C for 1 hour. The Pt counter electrodes were produced by thermal deposition of 20 mM chloroplatinic acid hexahydrate in isopropanol onto the FTO glasses at 450 °C for 0.5 hour. The resulting TiO₂ electrodes were immersed in the commercial N719 dye solution (0.3 mM in ethanol) for 12 hours. The sensitization of the organic dyes on TiO₂ photoanodes was performed in 0.3 mM dye solution for 12 hours. The iodine-based electrolyte composed of 0.3 M 1,2-dimethyl-3-propylimidazolium iodide (DMPII), 0.1 M LiI, 0.05 M I₂, and 0.5 M 4-*tert*-butylpyridine in acetonitrile (ACN) was used. The solar cells were fabricated into a sandwich-type structure and illuminated by a standard solar simulator

(XM-500W, Trusttech) under a standard 100 mW cm^{-2} irradiation, which was calibrated by a standard silicon solar cell (91150V, Newport). The incident photon-to-current conversion efficiency (IPCE) was tested by an IPCE system (QTest 2000). The current-voltage (J - V) characteristic curves of the DSSC under simulated irradiation were recorded by an electrochemical workstation (CHI660E, CH Instrument).

2.3. Synthesis

2.3.1. Synthesis of compound **1**

(4,4'-(benzo[*c*][1,2,5]thiadiazole-4,7-diyl)bis(*N,N*-diphenylaniline))

A mixture of 4,7-dibromo-2,1,3-benzothiadiazole (400 mg, 1.36 mmol), 4-(diphenylamino)phenylboronicacid (983 mg, 3.40 mmol), Pd(dppf)Cl₂ (55 mg, 0.07 mmol), K₂CO₃ (1.89 g, 13.6 mmol), toluene (24 mL) and DMF (8 mL) was refluxed under a N₂ atmosphere for 20 hours. The mixture was poured into water and extracted with DCM. After the organic phase was washed with water thoroughly and it was dried over anhydrous Na₂SO₄. The solvent was removed under vacuum, and then the crude product was purified by silica-gel column chromatography using DCM/PE (1:4) as the eluent and the compound **1** as a red solid was obtained (yield: 95.3%). Mp 242–244 °C. IR (KBr) ν : 2955, 2923, 2853, 1588, 1480, 1400, 1384, 1314, 1274, 1180, 1076, 1027, 884, 822, 752, 695, 620, 512 cm^{-1} . ¹H NMR (400 MHz, CDCl₃) δ 7.88 (d, J = 8.7 Hz, 4H), 7.74 (s, 2H), 7.30 (t, J = 7.8 Hz, 8H), 7.21 (t, J = 8.6 Hz, 12H), 7.07 (t, J = 7.3 Hz, 4H). ¹³C NMR (100 MHz, CDCl₃) δ 154.17, 147.99, 147.51, 132.19, 131.02, 129.90, 129.36, 127.45, 124.90, 123.30, 122.95. HR-MS (ESI): m/z

[M+H]⁺ calcd for C₄₂H₃₁N₄S, 623.2264; found, 623.2250.

2.3.2. Synthesis of 3

(4,4'-(8-bromo-6*H*-indolo[2,3-*b*]quinoxaline-1,4-diyl)bis(*N,N*-diphenylaniline))

A mixture of **1** (400 mg, 0.64 mmol), zinc granule (2.00 g, 30.6 mmol), hydrochloric acid (36%, 10 mL), CHCl₃ (20 mL) and EtOH (10 mL) was refluxed under a N₂ atmosphere for 3 hours. The mixture was poured into water and extracted with CH₂Cl₂. After being washed with water thoroughly, the organic phase was separated and dried over anhydrous Na₂SO₄. After the solvent was removed, the compound **2** was obtained and used directly for the next reaction without further purification because it was sensitive to air.

Then the product with 6-bromoisatin (145 mg, 0.64mmol), *p*-toluenesulfonic acid (200 mg) and toluene (40 mL) was refluxed at 140 °C for 4 hours. The mixture was poured into water and extracted with CH₂Cl₂. The organic phase washed with water and dried over anhydrous Na₂SO₄. After the solvent was removed under vacuum, the product was mixed with potassium *tert*-butoxide (215 mg, 1.92 mmol), tetrabutyl ammonium bromide (100 mg, 0.31 mmol) and THF (20 mL) and stirred at room temperature for 1 hour before 2-ethylhexyl bromide (367 mg, 1.92 mmol) was added to the reaction mixture. The mixture was refluxed for 2 hours at 80 °C before being poured into water and extracted with CH₂Cl₂. After being washed with water thoroughly, the combined organic phase was dried over anhydrous Na₂SO₄ and the solvent was removed under vacuum. The crude product was purified by silica-gel column chromatography using DCM/PE (1:2) as the eluent and the compound **3** as a

yellow solid was obtained (yield: 77.9%). Mp 203–205 °C. IR (KBr) ν : 2956, 2923, 2852, 1594, 1511, 1493, 1404, 1314, 1277, 1192, 1178, 1063, 821, 752, 695, 510 cm^{-1} . ^1H NMR (400 MHz, CDCl_3) δ 8.28 (d, $J = 8.2$ Hz, 1H), 7.91 (d, $J = 7.5$ Hz, 1H), 7.88–7.72 (m, 5H), 7.65–7.60 (m, 1H), 7.48 (dd, $J = 8.2, 1.4$ Hz, 1H), 7.38–7.22 (m, 20H), 7.09 (q, $J = 7.1$ Hz, 4H), 4.37–4.17 (m, 2H), 1.48–1.26 (m, 7H), 1.25–1.19 (m, 2H), 0.94–0.89 (m, 3H), 0.82 (t, $J = 7.1$ Hz, 3H). ^{13}C NMR (100 MHz, CDCl_3) δ 147.90, 147.85, 147.19, 146.91, 145.64, 144.96, 139.39, 138.74, 137.86, 137.80, 137.63, 133.53, 133.24, 131.95, 131.77, 129.30, 129.25, 129.03, 126.54, 124.73, 124.38, 124.11, 123.74, 123.18, 122.96, 122.89, 122.80, 118.79, 112.89, 45.88, 38.46, 30.66, 28.41, 23.94, 23.01, 13.98, 10.43. HR-MS (ESI): m/z $[\text{M}+\text{H}]^+$ calcd for $\text{C}_{58}\text{H}_{51}\text{BrN}_5$, 896.3322; found, 896.3307.

2.3.3. Synthesis of compound 4 (5-(1,4-bis(4-(diphenylamino)phenyl)-6-(2-ethylhexyl)-6H-indolo[2,3-b]quinoxalin-8-yl)thiophene-2-carbaldehyde)

A mixture of **3** (310 mg, 0.35 mmol), 5-formyl-2-thiopheneboronic acid (135 mg, 0.87 mmol), $\text{Pd}(\text{dppf})\text{Cl}_2$ (30 mg, 0.04 mmol), K_2CO_3 (500 mg, 1.73 mmol), toluene (40 mL) and DMF (8 mL) was stirred under a N_2 atmosphere for 4 hours at 80 °C. Then the mixture was poured into water and extracted with CH_2Cl_2 . After being washed with water thoroughly, the organic phase was separated and dried over anhydrous Na_2SO_4 . The crude product was purified by silica-gel column chromatography using DCM/PE (1:1) as the eluent and the compound **4** as a red solid was obtained (yield: 88.9%). Mp 118–120 °C. IR (KBr) ν : 2956, 2923, 2852, 1669,

1593, 1510, 1492, 1466, 1409, 1314, 1275, 1217, 1178, 1019, 821, 753, 695, 669, 504 cm^{-1} . ^1H NMR (400 MHz, CDCl_3) δ 9.94 (s, 1H), 8.43 (d, $J = 8.1$ Hz, 1H), 7.89 (d, $J = 7.5$ Hz, 1H), 7.87–7.73 (m, 6H), 7.70 (s, 1H), 7.66 (s, 1H), 7.57 (d, $J = 3.9$ Hz, 1H), 7.36–7.30 (m, 6H), 7.29–7.19 (m, 14H), 7.12–7.00 (m, 4H), 4.40–4.24 (m, 2H), 1.43–1.34 (m, 5H), 1.28–1.23 (m, 6H), 0.93–0.88 (m, 3H), 0.79 (t, $J = 7.2$ Hz, 3H). ^{13}C NMR (100 MHz, CDCl_3) δ 182.76, 154.20, 147.90, 147.86, 147.21, 146.93, 145.49, 145.23, 143.07, 139.42, 138.86, 137.83, 137.76, 137.36, 134.99, 133.50, 133.25, 131.98, 131.78, 129.33, 129.28, 129.17, 126.55, 125.00, 124.75, 124.42, 123.71, 123.14, 123.00, 122.88, 122.84, 120.69, 118.90, 107.23, 45.75, 38.70, 29.74, 28.54, 24.06, 23.03, 14.01, 10.54. HR-MS (ESI): m/z $[\text{M}+\text{H}]^+$ calcd for $\text{C}_{63}\text{H}_{54}\text{N}_5\text{OS}$, 928.4044; found, 928.4027.

2.3.4. Synthesis of 5
(5-(1,4-bis(4-(diphenylamino)phenyl)-6-(2-ethylhexyl)-6H-indolo[2,3-b]quinoxalin-8-yl)furan-2-carbaldehyde)

The synthetic process of **5** resembles that of **4**. The crude product was purified by silica-gel column chromatography using DCM/PE (1:1) as the eluent and the compound **5** as a red solid was obtained (yield: 89.6%). Mp 116–118 °C. IR (KBr) ν : 2956, 2924, 2854, 1677, 1629, 1592, 1468, 1410, 1314, 1275, 1180, 1073, 1026, 972, 937, 821, 753, 695, 621, 512 cm^{-1} . ^1H NMR (400 MHz, CDCl_3) δ 9.76 (s, 1H), 8.47 (d, $J = 8.1$ Hz, 1H), 7.91 (d, $J = 7.5$ Hz, 2H), 7.89–7.82 (m, 3H), 7.8–7.76 (m, 3H), 7.42 (d, $J = 3.7$ Hz, 1H), 7.34 (d, $J = 7.4$ Hz, 6H), 7.31–7.23 (m, 14H), 7.12–7.05 (m, 4H), 4.44–4.31 (m, 2H), 1.44–1.38 (m, 4H), 1.29 (s, 7H), 0.91 (s, 3H), 0.81 (t, $J = 7.2$

Hz, 3H). ^{13}C NMR (100 MHz, CDCl_3) δ 177.29, 159.31, 152.42, 147.91, 147.87, 147.19, 146.92, 145.47, 145.11, 139.40, 138.87, 137.81, 137.74, 133.52, 133.29, 131.99, 131.79, 130.61, 129.32, 129.28, 129.15, 126.50, 125.33, 124.74, 124.43, 123.47, 123.13, 122.99, 122.89, 122.84, 120.76, 117.78, 109.05, 105.92, 45.80, 38.59, 29.75, 28.52, 24.07, 23.02, 14.01, 10.56. HR-MS (ESI): m/z $[\text{M}+\text{H}]^+$ calcd for $\text{C}_{63}\text{H}_{54}\text{N}_5\text{O}_2$, 912.4272; found, 912.4259.

2.3.5. Synthesis of compound QX22
((E)-3-(5-(1,4-bis(4-(diphenylamino)phenyl)-6-(2-ethylhexyl)-6H-indolo[2,3-b]quinoxalin-8-yl)thiophen-2-yl)-2-cyanoacrylic acid)

A mixture of compound **4** (90 mg, 0.097 mmol), cyanoacetic acid (41 mg, 0.49 mmol), $\text{CH}_3\text{CN}/\text{CHCl}_3$ (10/20 mL) and piperidine (0.5 mL) was stirred at 85 °C for 5 hours under a N_2 atmosphere. Then the mixture was poured into water and extracted with CH_2Cl_2 . After washed with water thoroughly, the organic phase was separated and dried over anhydrous Na_2SO_4 . The crude product was purified by silica-gel column chromatography using DCM/MeOH (15:1) as the eluent and the compound **QX22** as a red solid was obtained (yield: 94.2%). Mp 270–272 °C. IR (KBr) ν : 2955, 2924, 2854, 1629, 1593, 1509, 1493, 1458, 1399, 1384, 1276, 1180, 1081, 965, 820, 752, 696 cm^{-1} . ^1H NMR (400 MHz, $\text{DMSO}-d_6$) δ 8.13 (d, $J = 11.4$ Hz, 2H), 7.91–7.82 (m, 2H), 7.76 (d, $J = 8.1$ Hz, 2H), 7.74–7.61 (m, 5H), 7.57 (d, $J = 8.3$ Hz, 1H), 7.43–7.26 (m, 8H), 7.19–6.93 (m, 16H), 4.27–4.13 (m, 2H), 1.25–1.17 (m, 6H), 1.11–1.01 (m, 3H), 0.76 (t, $J = 7.2$ Hz, 3H), 0.65 (t, $J = 7.1$ Hz, 3H). ^{13}C NMR (100 MHz, $\text{DMSO}-d_6$) δ 152.40, 147.66, 146.65, 146.62, 145.23, 144.72, 142.98, 140.16,

139.17, 137.16, 135.86, 134.88, 134.49, 133.35, 133.18, 133.17, 132.15, 132.13, 132.06, 131.93, 131.91, 129.86, 129.75, 128.86, 124.79, 124.55, 124.35, 123.51, 123.38, 122.46, 122.41, 122.40, 122.34, 122.31, 122.28, 107.00, 106.98, 38.27, 30.46, 29.45, 28.21, 23.74, 22.89, 14.14, 10.59. HR-MS (ESI): m/z $[M+H]^+$ calcd for $C_{66}H_{55}N_6O_2S$, 995.4102; found, 995.4082.

2.3.6. Synthesis of compound QX23
((E)-3-(5-(1,4-bis(4-(diphenylamino)phenyl)-6-(2-ethylhexyl)-6H-indolo[2,3-b]quinoxalin-8-yl)furan-2-yl)-2-cyanoacrylic acid)

The synthetic process of **QX23** resembles that of **QX22**. The product was purified by silica-gel column chromatography using DCM/MeOH (15:1) as the eluent and the compound **QX23** as a red solid was obtained (yield: 93.6%). Mp 240–242 °C. IR (KBr) ν : 2956, 2924, 2854, 1594, 1551, 1511, 1493, 1467, 1395, 1314, 1276, 1187, 1075, 1025, 968, 821, 793, 752, 696, 617, 510 cm^{-1} . 1H NMR (400 MHz, DMSO- d_6) δ 8.15 (d, $J = 7.5$ Hz, 1H), 8.00 (s, 1H), 7.91 (s, 1H), 7.78–7.62 (m, 7H), 7.43–7.29 (m, 10H), 7.18–7.02 (m, 16H), 4.19–4.09 (m, 2H), 1.25 (d, $J = 13.3$ Hz, 6H), 1.03 (d, $J = 6.0$ Hz, 3H), 0.75 (t, $J = 7.1$ Hz, 3H), 0.62 (t, $J = 6.9$ Hz, 3H). ^{13}C NMR (100 MHz, DMSO- d_6) δ 153.81, 153.79, 152.41, 151.38, 149.56, 143.45, 142.84, 141.83, 140.62, 139.79, 138.11, 137.93, 136.96, 136.92, 136.72, 136.22, 134.64, 134.53, 131.77, 131.07, 129.58, 129.53, 129.30, 128.28, 128.25, 128.16, 127.22, 127.19, 127.17, 127.12, 127.08, 124.02, 123.98, 119.22, 115.95, 111.08, 110.80, 42.60, 34.76, 34.22, 32.66, 28.21, 27.65, 18.86, 15.20. HR-MS (ESI): m/z $[M+H]^+$ calcd for $C_{66}H_{55}N_6O_3$, 979.4330; found, 979.4314.

2.3.7. Synthesis of compound QX24

((Z)-2-(5-((5-(1,4-bis(4-(diphenylamino)phenyl)-6-(2-ethylhexyl)-6*H*-indolo[2,3-*b*]quinoxalin-8-yl)thiophen-2-yl)methylene)-4-oxothiazolidin-2-ylidene)malononitrile)

A mixture of compound **5** (55 mg, 0.059 mmol), 2-(4-oxothiazolidin-2-ylidene)malononitrile (30 mg, 0.18 mmol), ethanol/CHCl₃ (1:2, 30 mL) and 10 drops of NaOH (20%) was refluxed at 80 °C for 10 hours under a N₂ atmosphere. Then the mixture was poured into water and extracted with CH₂Cl₂. After being washed with water thoroughly, the organic phase was separated and dried over anhydrous Na₂SO₄. The crude product was purified by silica-gel column chromatography using DCM/MeOH (15:1) as the eluent and the compound **QX24** as a red solid was obtained (yield: 95.5%). Mp > 300 °C. IR (KBr) v: 2956, 2924, 2853, 1654, 1637, 1593, 1491, 1459, 1400, 1384, 1313, 1276, 1185, 1081, 1025, 821, 754, 698 cm⁻¹. ¹H NMR (400 MHz, DMSO-*d*₆) δ 8.21 (d, *J* = 8.1 Hz, 1H), 8.00 (s, 1H), 7.90 (d, *J* = 3.6 Hz, 1H), 7.85 (d, *J* = 7.5 Hz, 1H), 7.82–7.66 (m, 7H), 7.62 (d, *J* = 3.7 Hz, 1H), 7.44–7.30 (m, 8H), 7.23–7.00 (m, 16H), 4.38–4.24 (m, 2H), 1.30 (s, 5H), 1.22–1.14 (m, 2H), 1.10 (d, *J* = 6.4 Hz, 2H), 0.83 (t, *J* = 7.2 Hz, 3H), 0.69 (t, *J* = 7.2 Hz, 3H). ¹³C NMR (100 MHz, DMSO-*d*₆) δ 185.03, 183.25, 178.97, 152.40, 152.37, 151.64, 151.43, 150.37, 149.84, 145.05, 143.56, 142.94, 142.50, 141.92, 140.58, 139.00, 138.12, 138.02, 136.98, 136.80, 134.81, 134.69, 133.46, 131.83, 131.26, 129.57, 129.28, 128.45, 128.30, 127.36, 127.15, 125.94, 125.09, 123.55, 123.02, 121.65, 111.58, 99.99, 84.39, 53.70, 43.03, 35.32, 32.85, 27.62, 22.44, 18.95, 15.45.

HR-MS (ESI): m/z $[M-H]^-$ calcd for $C_{69}H_{53}N_8OS_2$, 1073.3789; found, 1073.3785.

2.3.8. Synthesis of compound QX25

((Z)-2-(5-((5-(1,4-bis(4-(diphenylamino)phenyl)-6-(2-ethylhexyl)-6H-indolo[2,3-b]quinoxalin-8-yl)furan-2-yl)methylene)-4-oxothiazolidin-2-ylidene)malononitrile)

The synthetic process of compound **QX25** resembles that of compound **QX24** and the crude product was purified by silica-gel column chromatography using DCM/MeOH (15:1) as the eluent and the compound **QX25** as a deep red solid was obtained (yield: 93.1%). Mp 226–228 °C. IR (KBr) ν : 2956, 2924, 2853, 1654, 1636, 1595, 1491, 1468, 1400, 1384, 1314, 1277, 1189, 1075, 1028, 968, 821, 751, 696 cm^{-1} . 1H NMR (400 MHz, DMSO- d_6) δ 8.24 (d, $J = 8.1$ Hz, 1H), 7.84 (s, 1H), 7.81–7.73 (m, 4H), 7.70 (dd, $J = 8.1, 3.1$ Hz, 3H), 7.42–7.31 (m, 11H), 7.17–7.06 (m, 16H), 4.22 (d, $J = 7.1$ Hz, 2H), 1.33–1.22 (m, 7H), 1.06–1.01 (m, 2H), 0.75 (t, $J = 7.3$ Hz, 3H), 0.63 (t, $J = 7.3$ Hz, 3H). ^{13}C NMR (100 MHz, DMSO- d_6) δ 191.48, 183.30, 160.60, 155.43, 152.39, 152.35, 151.54, 151.31, 149.91, 149.46, 143.52, 142.73, 142.17, 141.95, 141.72, 138.11, 137.71, 136.91, 136.68, 136.11, 134.75, 134.65, 131.28, 131.24, 129.63, 129.40, 129.09, 128.40, 128.30, 126.94, 124.00, 123.34, 122.41, 121.94, 121.22, 120.02, 116.35, 109.59, 84.40, 43.10, 36.35, 35.02, 34.22, 32.85, 27.63, 18.84, 15.35. HR-MS (ESI): m/z $[M+H]^+$ calcd for $C_{69}H_{55}N_8O_2S$, 1059.4163; found, 1059.4162.

3. Results and discussion

3.1. Dye synthesis

The syntheses of the four dyes **QX22–25** were conducted by a concise synthetic route which was displayed in Scheme 1. 2-(1,1-dicyanomethylene)rhodanine (DCRD) was synthesized according to previous literatures [47,48]. Suzuki cross-coupling reaction of 4-(diphenylamino)phenylboronic acid with 4,7-dibromo-2,1,3-benzothiadiazole produced the triphenylamine-modified compound **1**. After reduction of the compound **1** with zinc granule under an acidic condition, ortho-diaminobenzene derivative **2** was obtained, which was used directly for next procedure. Then, condensation reaction of **2** with 6-bromoindole-2,3-dione and subsequent alkylation reaction produced the triphenylamine-modified 6*H*-indolo[2,3-*b*]quinoxaline intermediate **3**. The compound **1** or **3** with 5-formylthiophene-2-boronic acid or 5-formylfuran-2-boronic acid gave the π -extended aldehydes **4** or **5**. The aldehydes **4** and **5** finally reacted with cyanoacetic acid or 2-(1,1-dicyanomethylene)rhodanine by Knoevenagel reaction to give these four dyes **QX22**, **QX23**, **QX24**, and **QX25**, respectively. The ^1H and ^{13}C NMR spectra of the new compounds are shown in the supporting information.

3.2. Optical and electrochemical characterization

The UV-vis absorption spectra of **QX22–25** in DCM solutions and on photoanode TiO_2 films are displayed in Fig. 2. The characteristic data are summarized in Table 1. The four dyes all exhibited three strong distinct absorption bands in DCM solutions. The two distinct absorption bands around 200–350 nm correspond to the localized aromatic π - π^* transitions or n - π^* transitions of the conjugated backbone. The

absorption bands in the low-energy region around 400–600 nm can be assigned to the intramolecular charge transfer (ICT) transition [49]. The maximum absorption peaks of dyes **QX22** and **QX23** with cyanoacetic acid as the anchoring group were at 428 and 438 nm, while the dyes **QX24** and **QX25** with 2-(1,1-dicyanomethylene)rhodanine as the anchoring group were shown obviously red shift by 34 nm and 38 nm compared to that of **QX22** and **QX23**, respectively. Meanwhile, the absorption peaks of **QX23** and **QX25** with a furan unit as the π -bridge were shown a slight red shift than that of **QX22** and **QX24** with a thiophene unit as the π -bridge. The molar extinction coefficients at λ_{\max} for **QX22–25** were 2.47×10^4 (428 nm), 2.74×10^4 (438 nm), 3.23×10^4 (462 nm), and $1.81 \times 10^4 \text{ M}^{-1} \text{ cm}^{-1}$ (476 nm), respectively. As shown in Fig. 2b, when the four dyes were adsorbed on photoanode TiO_2 films, the absorption ranges of the four dyes showed much more broader as compared to that of the corresponding absorption spectra in DCM solutions which may be caused by the aggregation of dye molecules and the interactions between the dye molecules and TiO_2 semiconductor [50].

To investigate the electrochemical performance of the four dyes, cyclic voltammetry (CV) measurements were tested in DCM solutions and calibrated against ferrocene (0.63 V *vs.* NHE) [51] with a 100 mV s^{-1} scan rate. The electrochemical data of the four dyes were displayed in Table 1. The highest occupied molecular orbitals (HOMOs) of **QX22–25** corresponding to their first oxidation potentials (E_{ox}) were 0.93, 0.96, 0.95, and 0.94 V (*vs.* NHE), respectively. The HOMO levels of these dyes are more positive than the redox potential of the iodine/triiodide electrolyte (0.4

V vs. NHE), which ensures the regeneration of oxidized dyes. The band gap energies (E_{0-0}) of these four dyes were 2.21, 2.19, 2.17, and 2.16 eV, respectively, which were calculated from the onsets of the absorption spectra of these dyes in DCM solutions. The lowest unoccupied molecular orbitals (LUMOs) of **QX22–25** calculated from the equation $E_{ox} - E_{0-0}$ were -1.28 , -1.23 , -1.22 , and -1.22 V (vs. NHE), respectively. Obviously, the LUMO levels of the four dyes are also more negative than the conduction band (CB) of the TiO₂ electrode (-0.5 V vs. NHE), which guarantees the procedure of electron injection from the dyes to CB of TiO₂.

3.3. Theoretical calculations

In order to deep research the optimized configurations and frontier molecular orbital electron distributions of the four dyes **QX22–25**, the density functional theory (DFT) calculations were performed by Gauss09w at B3LYP/6-31G* level. The optimized configurations and electron distributions of the four dyes are shown in Fig. 4. The optimized configurations show that each dye molecule present a T-shaped structure with two propeller-shaped triphenylamine moieties attaching on planar rigid indoloquinoxaline skeleton, which may be beneficial to suppress the intermolecular aggregation and improve photovoltage. As a result, these dyes with an indoloquinoxaline core combined with two triphenylamine moieties have a good balanced structure, which can adequately involve the advantages of indoloquinoxaline acceptor and triphenylamine donor. The dihedral angles between the π -bridge and indoloquinoxaline were calculated to be 29.1, 1.9, 28.2, and 1.5° for **QX22–25**,

respectively. Obviously, the dyes **QX22** and **QX24** based on the furan π -bridge has a much smaller dihedral angle than that of the dyes **QX23** and **QX25** based on the thiophene π -bridge. The smaller dihedral angles between the π -bridge and indoloquinoline acceptor can enhance the electron delocalization and transfer, and expand the absorption spectra. As shown in Fig. 4, the four dyes have the similar frontier molecular orbital distributions. The electron density of the HOMO and HOMO-1 states for these dyes is uniformly distributed on the two triphenylamine donors. On the other hand, the electron density of the LUMO states of the four dyes mainly locates through the cyanoacrylic acid/DCRD acceptors and their nearby π -bridge groups. While as for the LUMO+1 states of these dyes, the electron density mainly locates on the subordinate acceptor indoloquinoline and slightly locates on the π -bridges and cyanoacrylic acid/DCRD acceptors. This calculated result demonstrates the T-shaped structure with an indoloquinoline core as the subordinate acceptor and two triphenylamine moieties as the donors is beneficial to the electron transfer from HOMO/HOMO-1 to LUMO/LUMO+1 by photoexcitation.

3.4. Photovoltaic performance

The DSSC performances of the solar cells based on **QX22–25** under AM 1.5G (100 mW cm⁻²) irradiation were investigated using an iodine electrolyte composed of 0.3 M DMPII, 0.1 M LiI, 0.05 M I₂, and 0.5 M 4-*tert*-butyl pyridine in ACN. The active area of these assembled DSSCs was set as 0.16 cm² using a metal mask. As is known to all, the dye-bath solvents have significant influence on the photovoltaic

performances of organic dye-sensitized solar cells. The effects of different solvents such as dichloromethane (DCM), toluene (PhMe), trichloromethane (TCM), tetrahydrofuran (THF) and ethanol (EtOH) on the photovoltaic performance of DSSC devices based on the dye **QX22** were investigated and the results are shown in Table 2. The corresponding photocurrent density-voltage (J - V) curves are displayed in Fig. 5. Apparently, the cell using the photoanode sensitized in ethanol solution performed the highest short-circuit current density (J_{sc}) and the highest open-circuit voltage (V_{oc}) than that of those sensitized in other solutions, which resulted in the highest PCE, indicating EtOH is the appropriate solvent for these (D)₂-A- π -A type dyes. The photovoltaic performance data of DSSC devices based on other dyes **QX23–25** using different dye-bath solvents are also shown in the supporting information.

The J - V curves of the cells based on **QX22–25** are shown in Fig. 6. The cell performance parameters of **QX22–25** using commercial **N719** dye as a reference are displayed in Table 3. The overall PCEs of the four dyes lay in the range of 4.35–7.09%, with an order of **QX24** < **QX25** < **QX22** < **QX23**. The dye **QX23** with a cyanoacrylic acid anchoring group and a furan π -bridge exhibited a highest V_{oc} of 817 mV, a highest J_{sc} of 12.9 mA cm⁻², and a fill factor (FF) of 67.3%, generating a highest PCE of 7.09%. Finally, the PCE of **QX23**-based cell reached about 88% of the conventional Ru(II) dye **N719**-based cell (V_{oc} : 772 mV; J_{sc} : 15.8 mA cm⁻²; PCE: 8.10%) which was fabricated and measured under the same conditions. When the π -bridge group was changed to thiophene, the dye **QX22** presented a lower J_{sc} of 11.9

mA cm^{-2} , resulting in a lower PCE of 6.05% compared with **QX23**. As shown in Fig. 6, **QX24** and **QX25** with a DCRD anchoring group exhibited a relatively poorer DSSC performances (**QX24**: a V_{oc} of 707 mV, a J_{sc} of 9.03 mA cm^{-2} , and a PCE of 4.35%; **QX25**: a V_{oc} of 724 mV, a J_{sc} of 9.71 mA cm^{-2} , and a PCE of 4.81%) compared with **QX22** and **QX23** with a cyanoacrylic acid anchoring group. Obviously, the anchoring groups have a great effect on the DSSC performances of these dyes and the dye loading amount of **QX22** and **QX23** with a cyanoacrylic acid anchoring group was measured to be 121 and 130 nmol cm^{-2} , respectively. However, the adsorption amount of **QX24** and **QX25** with a DCRD anchoring group significantly decreased to 51.2 and $58.5 \text{ nmol cm}^{-2}$, respectively, which may be one of the reasons for the reduction of their J_{sc} values.

In order to investigate the reason of the different J_{sc} values of these four dyes, the incident photon-to-current conversion efficiency (IPCE) measurements of the solar cells sensitized by **QX22–25** have been performed. The IPCE spectra for all these cells exhibited a broad response within a wavelength range from 350 to 700 nm (Fig. 7), indicating that all the dyes can efficiently convert the visible light into photocurrent. The spectra onsets of **QX22–25** were at 690, 700, 710, and 720 nm, respectively. As shown in Fig 7, the cell sensitized by **QX23** had the highest IPCE response corresponding to its highest J_{sc} value of 12.9 mA cm^{-2} and gave over 60% IPCE values from 400 to 600 nm with a maximum of 83% at 450 nm. The highest and broadest IPCE response could explain its highest J_{sc} value in the J - V measurements.

3.5. Electrochemical impedance spectroscopy

Electrochemical impedance spectroscopy (EIS) measurements for the four dyes **QX22–QX25** were performed to research the electron recombination in DSSCs [52,53]. The corresponding Nyquist plots and Bode phase plots are shown in Fig. 8. These measurements were performed in a frequency range from 0.1 Hz to 100 kHz under a bias of -0.80 V in complete darkness. As displayed in Fig. 8a, the larger semicircle in the low-frequency region corresponds to the charge transfer resistance (R_{ct}) at the dyes/TiO₂/electrolyte interface [54,55]. The radius of this semicircle corresponds to the R_{ct} value and the larger R_{ct} value means the more efficient hindrance of electron recombination at the dyes/TiO₂/electrolyte interface, the decreased dark current and improved photovoltage [56,57]. The order of R_{ct} values is **QX24** (31.5 Ω) < **QX25** (38.4 Ω) < **QX22** (54.9 Ω) < **QX23** (80.0 Ω), which is consistent well with the V_{oc} values of **QX24** (707 mV) < **QX25** (724 mV) < **QX22** (797 mV) < **QX23** (817 mV).

Besides, the peaks of the lower frequency region in the Bode plots also comply with the order of V_{oc} values. The electron lifetime (τ) as another important parameter can be calculated from the equation $\tau = 1/(2\pi f)$, and the higher electron lifetime means the more efficient hinder of charge recombination at the dyes/TiO₂/electrolyte interface and higher photovoltage [59]. For the four dyes based devices, the calculated electron lifetime values increased in the order of **QX24** (10.8 ms) < **QX25** (13.1 ms)

< **QX22** (19.3 ms) < **QX23** (34.3 ms). On the basis of above studies, the best DSSC performance of **QX23** is mainly attributed to its significantly highest IPCE response (namely highest J_{sc}) and obviously smallest electron recombination rate (namely highest V_{oc}) compared with the other three dyes.

4. Conclusions

A series of metal-free organic sensitizers (**QX22–25**) based on triphenylamine and indoloquinoxaline have been successfully designed and synthesized as a T-shaped (D)₂–A– π –A type structure for DSSCs. Two triphenylamine donors were attached on an indoloquinoxaline-based subordinate acceptor. Different π -bridges such as thiophene and furan and acceptor/anchoring groups such as cyanoacrylic acid and 2-(1,1-dicyanomethylene)rhodanine were used to tune their photoelectrical properties. The corresponding optical, electrochemical, photovoltaic measurements as well as the DFT calculations have been systematically investigated to certify these dyes are all capable as photosensitizers. The dye **QX23** with a furan π -bridge and a cyanoacrylic acid acceptor/anchoring group have achieved a highest PCE of 7.09% with a J_{sc} of 12.9 mA cm⁻² and a V_{oc} of 817 mV, demonstrating it is a promising strategy to construct efficient (D)₂–A– π –A type sensitizers by incorporating indoloquinoxaline and triphenylamine.

Acknowledgments

We are very grateful to the National Natural Science Foundation of China (No:

21376054) and Project of Education Department of Fujian Province (No: JAT160052) for their generous financial support.

References

- [1] B. Pashaei, H. Shahroosvand, M. Grätzel, M.K. Nazeeruddin, Influence of Ancillary Ligands in Dye-Sensitized Solar Cells, *Chemical Reviews* 116 (2016) 9485–9564.
- [2] A. Hagfeldt, G. Boschloo, L.C. Sun, L. Kloo, H. Pettersson, Dye-Sensitized Solar Cells, *Chem. Rev.* 110 (2010) 6595–6663.
- [3] M. Urbani, M. Grätzel, M.K. Nazeeruddin, T. Torres, Meso-Substituted Porphyrins for Dye-Sensitized Solar Cells, *Chem. Rev.* 114 (2014) 12330–12396.
- [4] Z. Sun, M. Liang, J. Chen, Kinetics of Iodine-Free Redox Shuttles in Dye-Sensitized Solar Cells: Interfacial Recombination and Dye Regeneration, *Accounts. Chem. Res.* 48 (2015) 1541–1550.
- [5] J. Wu, Z. Lan, J. Lin, M. Huang, Y. Huang, L. Fan, G. Luo, Electrolytes in Dye-Sensitized Solar Cells, *Chem. Rev.* 115 (2015) 2136–2173.
- [6] M. Liang, J. Chen, Arylamine organic dyes for dye-sensitized solar cells, *Chemical Society Reviews* 42 (2013) 3453–3488.
- [7] Y. Xie, W. Wu, H. Zhu, J. Liu, W. Zhang, H. Tian, W.-H. Zhu, Unprecedentedly targeted customization of molecular energy levels with auxiliary-groups in organic solar cell sensitizers, *Chem. Sci.* 7 (2016) 544–549.
- [8] Y. Wang, B. Chen, W. Wu, X. Li, W. Zhu, H. Tian, Y. Xie, Efficient Solar Cells Sensitized by Porphyrins with an Extended Conjugation Framework and a Carbazole

Donor: From Molecular Design to Cosensitization, *Angew. Chem. Int. Ed.* 53 (2014) 10779–10783.

[9] T. Higashino, Y. Fujimori, K. Sugiura, Y. Tsuji, S. Ito, H. Imahori, Tropolone as a High-Performance Robust Anchoring Group for Dye-Sensitized Solar Cells, *Angew. Chem. Int. Ed.* 54 (2015) 9052–9056.

[10] T. Higashino, H. Imahori, Porphyrins as excellent dyes for dye-sensitized solar cells: recent developments and insights, *Dalton. Trans.* 44 (2015) 448–463.

[11] S. Mathew, A. Yella, P. Gao, R. Humphry-Baker, B.F.E. Curchod, N. Ashari-Astani, I. Tavernelli, U. Rothlisberger, M.K. Nazeeruddin, M. Grätzel, Dye-sensitized solar cells with 13% efficiency achieved through the molecular engineering of porphyrin sensitizers, *Nat. Chem.* 6 (2014) 242–247.

[12] Z. Yao, M. Zhang, R. Li, L. Yang, Y. Qiao, P. Wang, A Metal-Free N-Annulated Thienocyclopentaperylene Dye: Power Conversion Efficiency of 12% for Dye-Sensitized Solar Cells, *Angew. Chem. Int. Ed.* 54 (2015) 5994–5998.

[13] G.B. Bodedla, K.R.J. Thomas, M.-S. Fan, K.-C. Ho, Benzimidazole-Branched Isomeric Dyes: Effect of Molecular Constitution on Photophysical, Electrochemical, and Photovoltaic Properties, *J. Org. Chem.* 81 (2016) 640–653.

[14] P.P. Dai, L. Yang, M. Liang, H.H. Dong, P. Wang, C.Y. Zhang, Z. Sun, S. Xue, Influence of the Terminal Electron Donor in D–D– π –A Organic Dye-Sensitized Solar Cells: Dithieno[3,2-b:2',3'-d]pyrrole versus Bis(amine), *ACS Appl. Mater. Interfaces* 7 (2015) 22436–22447.

[15] A. Baheti, K.R.J. Thomas, C.-T. Li, C.-P. Lee, K.-C. Ho, Fluorene-Based

Sensitizers with a Phenothiazine Donor: Effect of Mode of Donor Tethering on the Performance of Dye-Sensitized Solar Cells, *ACS Appl. Mater. Interfaces* 7 (2015) 2249–2262.

[16] L. Yang, Z. Zheng, Y. Li, W. Wu, H. Tian, Z. Wang, *N*-Annulated perylene-based metal-free organic sensitizers for dye-sensitized solar cells, *Chem. Commun.* 51 (2015) 4842–4845.

[17] X. Zhang, Y. Xu, F. Giordano, M. Schreier, N. Pellet, Y. Hu, C. Yi, N. Robertson, J. Hua, S.M. Zakeeruddin, H. Tian, M. Grätzel, Molecular Engineering of Potent Sensitizers for Very Efficient Light Harvesting in Thin-Film Solid-State Dye-Sensitized Solar Cells, *J. Am. Chem. Soc.* 138 (2016) 10742–10745.

[18] J. Luo, Z. Wan, C. Jia, Y. Wang, X. Wu, X. Yao, Co-sensitization of Dithiafulvenyl-Phenothiazine Based Organic Dyes with N719 for Efficient Dye-Sensitized Solar Cells, *Electrochim. Acta* 211 (2016) 364–374.

[19] D.D. Babu, R. Su, A. El-Shafei, A.V. Adhikari, From Molecular Design to Co-sensitization; High performance indole based photosensitizers for dye-sensitized solar cells, *Electrochim. Acta* 198 (2016) 10–21.

[20] Z. Iqbal, W.-Q. Wu, Z.-S. Huang, L. Wang, D.-B. Kuang, H. Meier, D. Cao, Trilateral π -conjugation extensions of phenothiazine-based dyes enhance the photovoltaic performance of the dye-sensitized solar cells, *Dyes Pigm.* 124 (2016) 63–71.

[21] Z.-S. Huang, T. Hua, J. Tian, L. Wang, H. Meier, D. Cao, Dithienopyrrolobenzotriazole-based organic dyes with high molar extinction

coefficient for efficient dye-sensitized solar cells, *Dyes Pigm.* 125 (2016) 229–240.

[22] X. Li, Z. Zheng, W. Jiang, W. Wu, Z. Wang, H. Tian, New D–A– π –A organic sensitizers for efficient dye-sensitized solar cells, *Chem. Commun.* 51 (2015) 3590–3592.

[23] Z. Yao, M. Zhang, H. Wu, L. Yang, R. Li, P. Wang, Donor/Acceptor Indenoperylene Dye for Highly Efficient Organic Dye-Sensitized Solar Cells, *J. Am. Chem. Soc.* 137 (2015) 3799–3802.

[24] Y. Wang, C. Yang, J. Chen, H. Qi, J. Hua, Y. Liu, E. Baranoff, H. Tan, J. Fan, W. Zhu, Influence of the donor size in panchromatic D– π –A– π –A dyes bearing 5-phenyl-5H-dibenzo-[b,f]azepine units for dye-sensitized solar cells, *Dyes Pigm.* 127 (2016) 204–212.

[25] W. Zhang, Y. Wu, H. Zhu, Q. Chai, J. Liu, H. Li, X. Song, W.-H. Zhu, Rational Molecular Engineering of Indoline-Based D–A– π –A Organic Sensitizers for Long-Wavelength-Responsive Dye-Sensitized Solar Cells, *ACS Appl. Mater. Interfaces* 7 (2015) 26802–26810.

[26] X. Song, W. Zhang, X. Li, H. Jiang, C. Shen, W.-H. Zhu, Influence of ethynyl position on benzothiadiazole based D–A– π –A dye-sensitized solar cells: spectral response and photovoltage performance, *J. Mater. Chem. C* 4 (2016) 9203–9211.

[27] Y. Wu, W. Zhu, Organic sensitizers from D– π –A to D–A– π –A: effect of the internal electron-withdrawing units on molecular absorption, energy levels and photovoltaic performances, *Chem. Soc. Rev.* 42 (2013) 2039–2058.

[28] J. Yang, P. Ganesan, J. Teuscher, T. Moehl, Y.J. Kim, C. Yi, P. Comte, K. Pei,

T.W. Holcombe, M.K. Nazeeruddin, J. Hua, S.M. Zakeeruddin, H. Tian, M. Grätzel, Influence of the Donor Size in D- π -A Organic Dyes for Dye-Sensitized Solar Cells, *J. Am. Chem. Soc.* 136 (2014) 5722–5730.

[29] L. Wang, X. Yang, X. Wang, L. Sun, Novel organic dyes with anchoring group of quinoxaline-2,3-diol and the application in dye-sensitized solar cells, *Dyes Pigm.* 113 (2015) 581–587.

[30] Z.-S. Huang, X.-F. Zang, T. Hua, L. Wang, H. Meier, D. Cao, 2,3-Dipentylidithieno[3,2-f:2',3'-h]quinoxaline-Based Organic Dyes for Efficient Dye-Sensitized Solar Cells: Effect of π -Bridges and Electron Donors on Solar Cell Performance, *ACS Appl. Mater. Interfaces* 7 (2015) 20418–20429.

[31] L. Yang, Z. Yao, J. Liu, J. Wang, P. Wang, A Systematic Study on the Influence of Electron-Acceptors in Phenanthrocarbazole Dye-Sensitized Solar Cells, *ACS Appl. Mater. Interfaces* 8 (2016) 9839–9848.

[32] Y.-S. Yen, J.-S. Ni, W.-I. Hung, C.-Y. Hsu, H.-H. Chou, J.-T.s. Lin, Naphtho[2,3-c][1,2,5]thiadiazole and 2H-Naphtho[2,3-d][1,2,3]triazole-Containing D-A- π -A Conjugated Organic Dyes for Dye-Sensitized Solar Cells, *ACS Appl. Mater. Interfaces* 8 (2016) 6117–6126.

[33] E. Wang, Z. Yao, Y. Zhang, G. Shao, M. Zhang, P. Wang, Significant Influences of Elaborately Modulating Electron Donors on Light Absorption and Multichannel Charge-Transfer Dynamics for 4-(Benzo[c][1,2,5]thiadiazol-4-ylethynyl)benzoic Acid Dyes, *ACS Appl. Mater. Interfaces* 8 (2016) 18292–18300.

[34] C.-L. Wang, M. Zhang, Y.-H. Hsiao, C.-K. Tseng, C.-L. Liu, M. Xu, P. Wang,

C.-Y. Lin, Porphyrins bearing a consolidated anthryl donor with dual functions for efficient dye-sensitized solar cells, *Energy Environ. Sci.* 9 (2016) 200–206.

[35] J.-S. Ni, Y.-C. Yen, J.T. Lin, Organic dyes with a fused segment comprising benzotriazole and thieno[3,2-b]pyrrole entities as the conjugated spacer for high performance dye-sensitized solar cells, *Chem. Commun.* 51 (2015) 17080–17083.

[36] Y. Tang, Y. Wang, X. Li, H. Agren, W.-H. Zhu, Y. Xie, Porphyrins Containing a Triphenylamine Donor and up to Eight Alkoxy Chains for Dye-Sensitized Solar Cells: A High Efficiency of 10.9%, *ACS Appl. Mater. Interfaces* 7 (2015) 27976–27985.

[37] H. Zhu, Y. Wu, J. Liu, W.W. Zhang, W. Wu, W.-H. Zhu, D–A– π –A featured sensitizers containing an auxiliary acceptor of benzoxadiazole: molecular engineering and co-sensitization, *J. Mater. Chem. A* 3 (2015) 10603–10609.

[38] S. Qu, C. Qin, A. Islam, Y. Wu, W. Zhu, J. Hua, H. Tian, L. Han, A novel D–A– π –A organic sensitizer containing a diketopyrrolopyrrole unit with a branched alkyl chain for highly efficient and stable dye-sensitized solar cells, *Chem. Commun.* 48 (2012) 6972–6974.

[39] F. Guo, X. Liu, Y. Ding, F. Kong, W. Chen, L. Zhou, S. Dai, Broad spectral-response organic D–A– π –A sensitizer with pyridine-diketopyrrolopyrrole unit for dye-sensitized solar cells, *RSC Adv.* 6 (2016) 13433–13441.

[40] Z. Chai, S. Wan, C. Zhong, T. Xu, M. Fang, J. Wang, Y. Xie, Y. Zhang, A. Mei, H. Han, Q. Peng, Q. Li, Z. Li, Conjugated or Broken: The Introduction of Isolation Spacer ahead of the Anchoring Moiety and the Improved Device Performance, *ACS Appl. Mater. Interfaces* 8 (2016) 28652–28662.

- [41] S. Chaurasia, J.-S. Ni, W.-I. Hung, J.T. Lin, *2H*-[1,2,3]Triazolo[4,5-*c*]pyridine Cored Organic Dyes Achieving a High Efficiency: a Systematic Study of the Effect of Different Donors and π Spacers, *ACS Appl. Mater. Interfaces* 7 (2015) 22046–22057.
- [42] N.P. Liyanage, A. Yella, M. Nazeeniddin, M. Grätzel, J.H. Delcamp, Thieno 3,4-*b* pyrazine as an Electron Deficient π -Bridge in D–A– π –A DSCs, *ACS Appl. Mater. Interfaces* 8 (2016) 5376–5384.
- [43] Y.-J. Chen, Y.-C. Chang, L.-Y. Lin, W.-C. Chang, S.-M. Chang, Enhancing the Spectral Response of Mesoporous ZnO Films of Dye-sensitized Solar Cells by Incorporating Metal-free Organic Sensitizer and N719 dye, *Electrochim. Acta* 178 (2015) 414–419.
- [44] K.R.J. Thomas, P. Tyagi, Synthesis, Spectra, and Theoretical Investigations of the Triarylamines Based on 6H-Indolo[2,3-*b*]quinoxaline, *J. Org. Chem.* 75 (2010) 8100–8111.
- [45] P. Tyagi, A. Venkateswararao, K.R.J. Thomas, Solution Processable Indoloquinoxaline Derivatives Containing Bulky Polyaromatic Hydrocarbons: Synthesis, Optical Spectra, and Electroluminescence, *J. Org. Chem.* 76 (2011) 4571–4581.
- [46] X. Qian, X. Wang, L. Shao, H. Li, R.C. Yan, L. Hou, Molecular engineering of D–D– π –A type organic dyes incorporating indoloquinoxaline and phenothiazine for highly efficient dye sensitized solar cells, *J. Power Sources* 326 (2016) 129–136.
- [47] J. Mao, N. He, Z. Ning, Q. Zhang, F. Guo, L. Chen, W. Wu, J. Hua, H. Tian, Stable Dyes Containing Double Acceptors without COOH as Anchors for Highly

Efficient Dye-Sensitized Solar Cells, *Angew. Chem. Int. Ed.* 51 (2012) 9873–9876.

[48] J. Mao, X. Zhang, S.-H. Liu, Z. Shen, X. Li, W. Wu, P.-T. Chou, J. Hua, Molecular engineering of D–A– π –A dyes with 2-(1,1-dicyanomethylene)rhodanine as an electron-accepting and anchoring group for dye-sensitized solar cells, *Electrochim. Acta* 179 (2015) 179–186.

[49] X.-X. Dai, H.-L. Feng, Z.-S. Huang, M.-J. Wang, L. Wang, D.-B. Kuang, H. Meier, D. Cao, Synthesis of phenothiazine-based di-anchoring dyes containing fluorene linker and their photovoltaic performance, *Dyes Pigm.* 114 (2015) 47–54.

[50] D. Kumar, K.R.J. Thomas, C.-P. Lee, K.-C. Ho, Organic Dyes Containing Fluorene Decorated with Imidazole Units for Dye-Sensitized Solar Cells, *J. Org. Chem.* 79 (2014) 3159–3172.

[51] P. Gao, H.N. Tsao, M. Grätzel, M.K. Nazeeruddin, Fine-tuning the Electronic Structure of Organic Dyes for Dye-Sensitized Solar Cells, *Org. Lett.* 14 (2012) 4330–4333.

[52] J. Zhang, F. Lu, S. Qi, Y. Zhao, K. Wang, B. Zhang, Y. Feng, Influence of various electron-donating triarylamine groups in BODIPY sensitizers on the performance of dye-sensitized solar cells, *Dyes Pigm.* 128 (2016) 296–303.

[53] X. Qian, L. Shao, H. Li, R.C. Yan, X. Wang, L. Hou, Indolo[3,2-b]carbazole-based multi-donor– π –acceptor type organic dyes for highly efficient dye-sensitized solar cells, *J. Power Sources* 319 (2016) 39–47.

[54] G. Wu, R. Kaneko, Y. Zhang, Y. Shinozaki, K. Sugawa, A. Islam, L. Han, I. Bedja, R.K. Gupta, Q. Shen, J. Otsuki, Neutral and anionic tetrazole-based ligands in

designing novel ruthenium dyes for dye-sensitized solar cells, *J. Power Sources* 307 (2016) 416–425.

[55] X. Qian, R. Yan, C. Xu, L. Shao, H. Li, L. Hou, New efficient organic dyes employing indeno[1,2-b]indole as the donor moiety for dye-sensitized solar cells, *J. Power Sources* 332 (2016) 103–110.

[56] J.-S. Ni, Y.-C. Yen, J.T. Lin, Organic sensitizers with a rigid dithienobenzotriazole-based spacer for high-performance dye-sensitized solar cells, *J. Mater. Chem. A* 4 (2016) 6553–6560.

[57] X. Qian, R. Yan, L. Shao, H. Li, X.Y. Wang, L. Hou, Triindole-modified push-pull type porphyrin dyes for dye-sensitized solar cells, *Dyes Pigm.* 134 (2016) 434–441.

[58] R. Misra, R. Maragani, D. Arora, A. Sharma, G.D. Sharma, Positional isomers of pyridine linked triphenylamine-based donor-acceptor organic dyes for efficient dye-sensitized solar cells, *Dyes Pigm.* 126 (2016) 38–45.

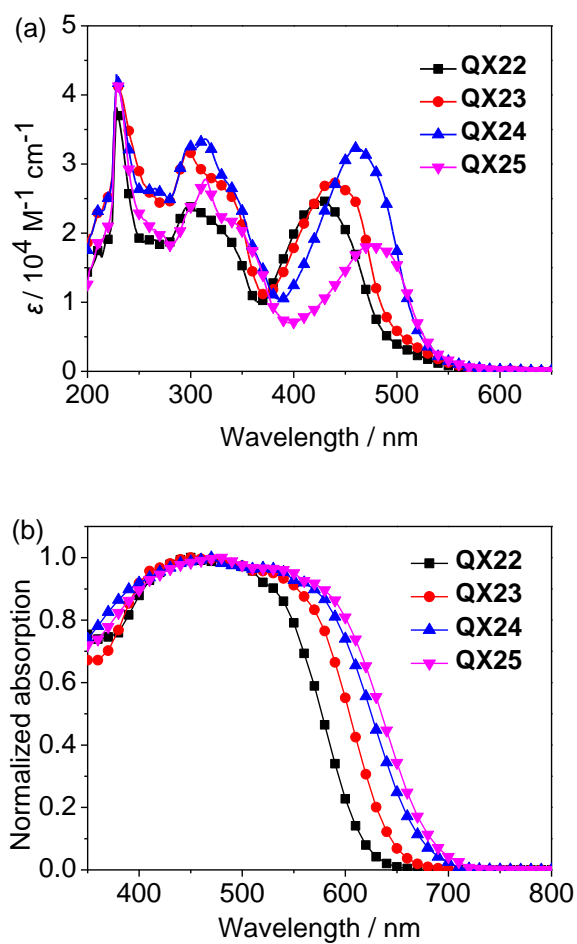


Fig. 2. UV-vis absorption spectra of **QX22–25** (a) in DCM solutions and (b) adsorbed on photoanode TiO_2 films.

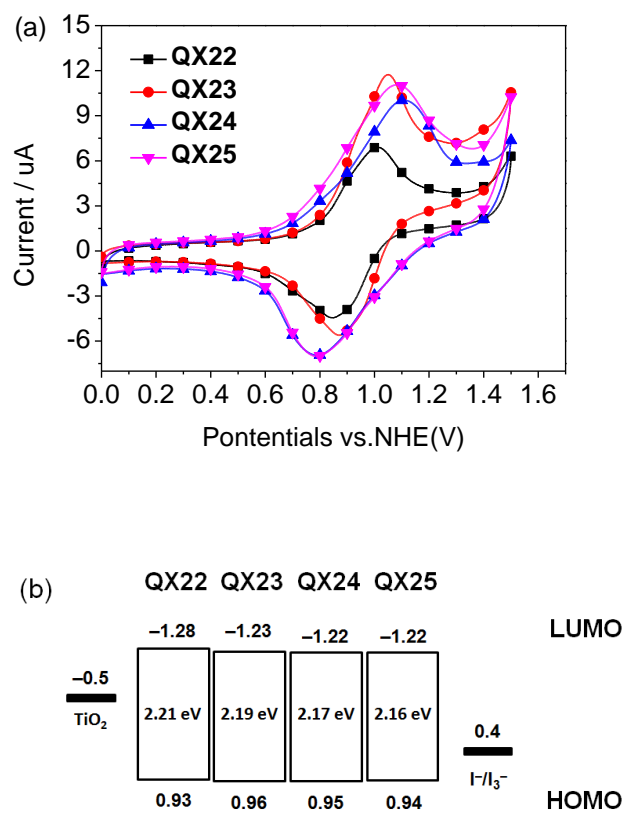


Fig. 3 (a) CV curves and (b) energy diagram of HOMO and LUMO levels for QX22–25 (V vs. NHE).

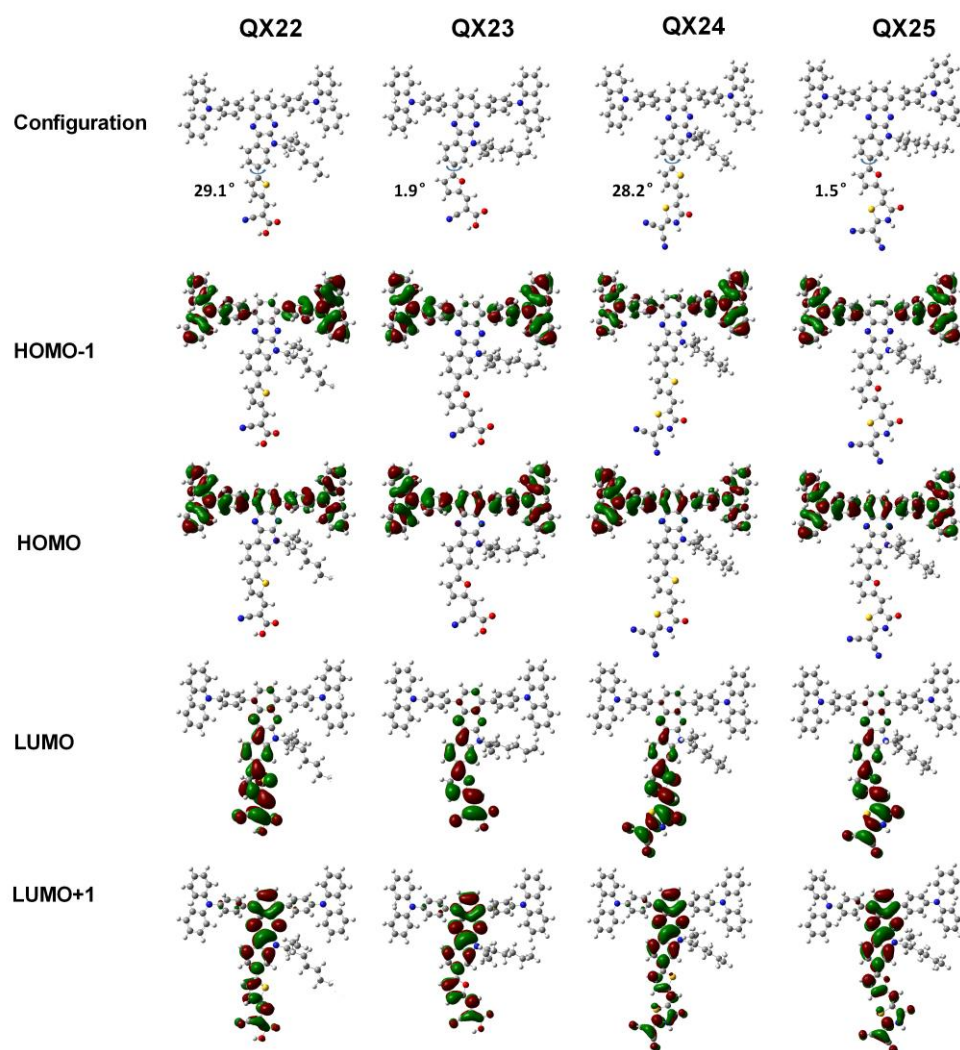


Fig. 4. The optimized configurations and frontier molecular orbital distributions of these four dyes **QX22–25** optimized by DFT at the B3LYP/6-31G* level.

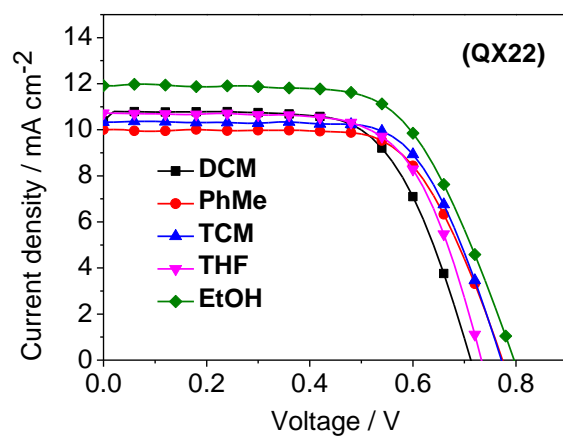


Fig. 5. The J - V curves of the DSSCs based on **QX22** using different dye-bath solvents.

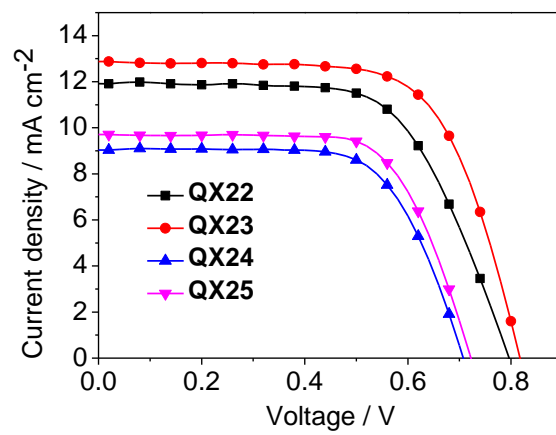


Fig. 6. The J - V curves of the solar cells based on **QX22–25**.

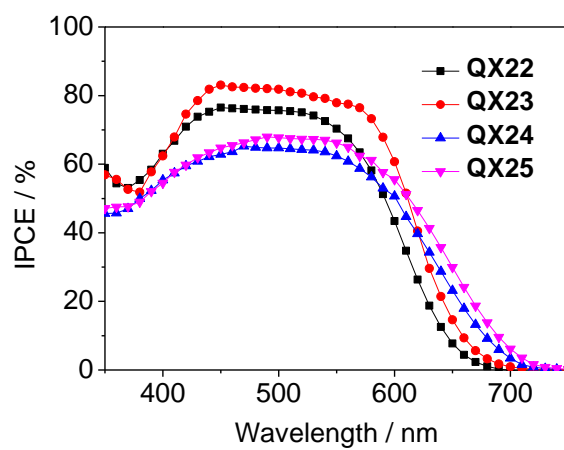


Fig. 7. IPCE spectra of the solar cells based on the four dyes **QX22–25**.

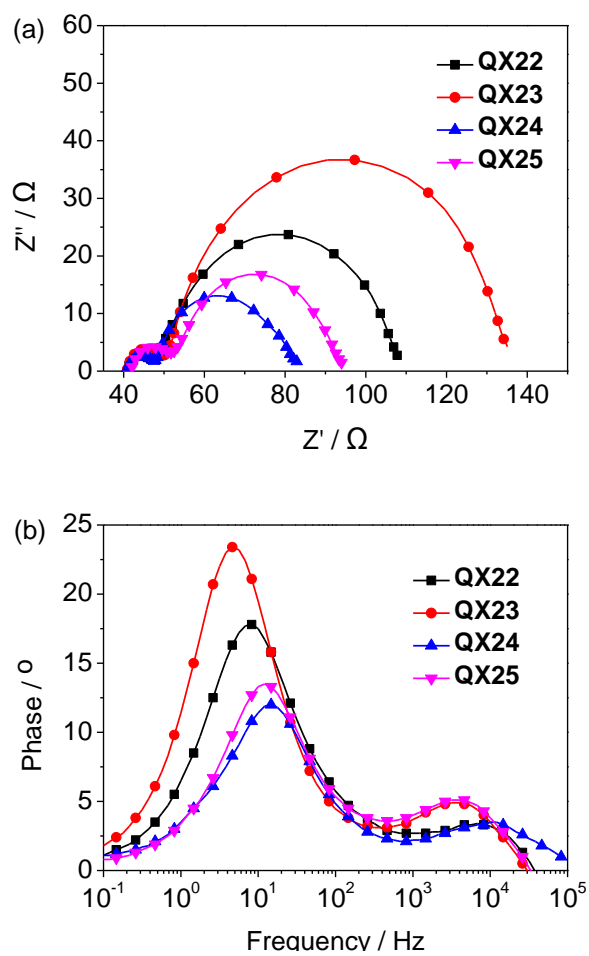
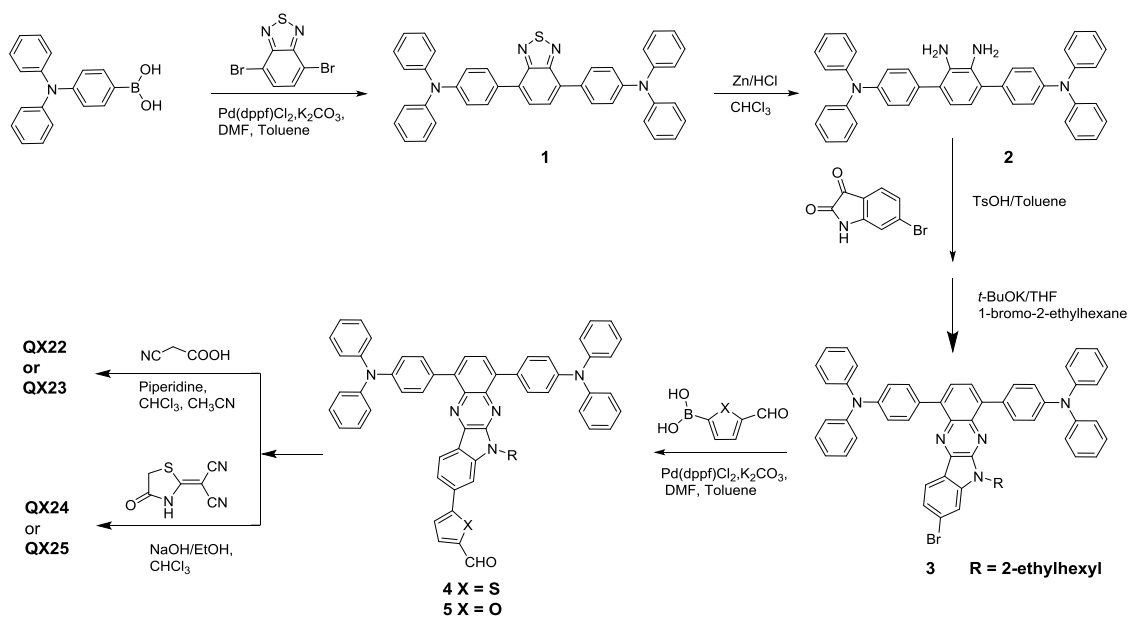


Fig. 8. (a) The Nyquist plots and (b) Bode phase plots for DSSCs based on QX22–QX25 under a bias of -0.80 V.



Scheme 1. Synthetic routes of the four dyes **QX22–25**.

Table 1 Optical and electrochemical data of **QX22–25**.^a

Dye	λ_{\max} (nm)	ε (10^4 M^{-1}	λ_{\max} (on TiO_2 ,	E_{ox} (V)	E_{0-0} (V)	E_{red} (V)
		cm^{-1})	nm)			
QX22	428	2.47	412	0.93	2.21	-1.28
QX23	438	2.74	420	0.96	2.19	-1.23
QX24	462	3.23	460	0.95	2.17	-1.22
QX25	476	1.81	472	0.94	2.16	-1.22

^a First oxidation potentials (vs. NHE) in DCM were calibrated with ferrocene (0.63 V vs. NHE); E_{0-0} values were estimated from the onsets of absorption spectra; $E_{\text{red}} = E_{\text{ox}} - E_{0-0}$.

Table 2 Photovoltaic data of **QX22** using different dye-bath solvents.

Dye-bath		V_{oc} (mV)	J_{sc} (mA cm ⁻²)	FF (%)	PCE (%)
Dye	solvent				
QX22	DCM	712	10.8	65.2	5.02
QX22	PhMe	774	10.0	67.1	5.19
QX22	TCM	769	10.3	68.7	5.44
QX22	THF	732	10.7	66.9	5.24
QX22	EtOH	797	11.9	63.8	6.05

Table 3 Photovoltaic data of **QX22–25** using commercial **N719** dye as a reference.^a

	Dye-bath	Dye loading	V_{oc}	J_{sc} (mA	FF	PCE
Dye	solvent	(nmol cm ⁻²)	(mV)	cm ⁻²)	(%)	(%)
QX22	EtOH	121	797	11.9	63.8	6.05
QX23	EtOH	130	817	12.9	67.3	7.09
QX24	EtOH	51.2	707	9.03	68.1	4.35
QX25	EtOH	58.5	724	9.71	68.4	4.81
N719	EtOH	--	772	15.8	66.4	8.10